Beyond the particular case of circuits with geometrically distributed components for approximation of fractional order models: Application to a new class of model for power law type long memory behaviour modelling

Jocelyn Sabatier

Beyond the particular case of circuits with geometrically distributed components for approximation of fractional order models: application to a new class of model for power law type long memory behaviour modelling

Jocelyn SABATIER,
IMS laboratory, Bordeaux University, UMR CNRS 5218, 351 Cours de la liberation, 33400 Talence, France
(e-mail: Jocelyn.sabatier@u-bordeaux.fr).

Abstract – In the literature, fractional models are commonly approximated by transfer functions with a geometric distribution of poles and zeros, or equivalently, using electrical Foster or Cauer type networks with components whose values also meet geometric distributions. This paper first shows that this geometric distribution is only a particular distribution case and that many other distributions (an infinity) are in fact possible. From the networks obtained, a class of partial differential equations (heat equation with a spatially variable coefficient) is then deduced. This class of equations is thus another tool for power law type long memory behaviour modelling, that solves the drawback inherent in fractional heat equations that was proposed to model anomalous diffusion phenomena.

Keywords: Power law type long memory behaviours, fractional models, Cauer networks, Foster networks, heat equation, poles and zeros geometric distributions.

1 - Introduction

It is well known that the diffusion equation of the form

$$\frac{\partial \phi(x,t)}{\partial t} = D_f \frac{\partial^2 \phi(x,t)}{\partial x^2} \tag{1}$$

produces power law type long memory behaviours of order 0.5 (D_f is a diffusion coefficient). That is why the Warburg impedance, defined in the frequency domain (variable ω) by $Z(j\omega) = (j\omega)^{-1/2}$, was introduced to model numerous diffusion-controlled processes in many domains such as electrochemistry (Warburg, 1901) (Randles, 1947), (Vetter, 1967), (Sluythers-Rehbach and Sluythers, 1984), (Bisquert et al., 1999), solid-state electronics and ionics (Lindmayer and Wrigley, 1965), (Van Herle and McEvoy, 1994), (Bisquert and Garcia-Belmonte, 1997). However, it is also well-known that there are processes whose behaviour cannot be modelled by the Warburg impedance as they exhibit a power law type behaviour of the form

$$Z(j\omega) = (j\omega)^{-\nu} \qquad 0 < \nu < 1 \qquad \nu \in \mathbb{R} \tag{2}$$

at least in a limited frequency range. These behaviours are connected to anomalous diffusion-based processes (Evangelista and Lenzi, 2018). To model this kind of behaviour, "fractionalizations" of the diffusion equation were introduced (Bisquert and Compte, 2001). These fractional (in time) diffusion equations are defined by

$$\frac{\partial^\nu \phi(x,t)}{\partial t^\nu} = D_f \frac{\partial^2 \phi(x,t)}{\partial x^2} \qquad 0 < \nu < 1. \tag{3}$$

However, this class of equations has similar drawbacks to those recently highlighted for fractional differential equations (Sabatier, 2020.b) (Sabatier et al., 2020.c) and for the

resulting fractional models such as pseudo state space descriptions (Sabatier et al., 2014). First, in relation (3), the fractional differentiation operator $\frac{\partial^\nu}{\partial t^\nu}$ is not defined uniquely. More than 30 definitions were listed in (De Oliveira and Tenreiro Machado, 2014). Results presented in the literature are obtained by choosing the most convenient definition to obtain them. In most cases, it is the Caputo definition that is chosen, as it can take into account the initial conditions without taking into account all the past of the system. However it was demonstrated in (Sabatier et al., 2010) (Sabatier and Farges, 2018) that all the system past ($t \to -\infty$) must be taken into account to ensure a proper initialisation, thus leading to difficulties in the definition of this past. This reflects the fact that the fractional differentiation operator $\frac{\partial^\nu}{\partial t^\nu}$ (but also the fractional integration operator) has an infinite memory, and exhibits infinitely slow and infinitely fast time constants. Such a situation excludes the possibility of linking the model internal variables to physical variables, even if fractional models remain accurate fitting models. Along the same lines, there is no proof for the physical meaning of parameter units associated to relation (3) (parameter D_f). To conclude this list of drawbacks, fractional differentiation and fractional integration operators are defined using singular kernels (Sabatier et al., 2019) (Sabatier, 2020.b), thus leading to difficulties in the solution / simulation of the fractional diffusion equation (3).

For all these reasons, alternative models must be found to model anomalous diffusion processes that exhibit power law type long memory behaviours, as was done recently for fractional differential equations (Sabatier et al., 2020.c) (Tartaglione et al., 2020). To reach this goal, this paper first reminds several solution that can be found in the literature for the approximation of fractional integration operator. The approximation based on a transfer function whose poles and zeros (frequency modes) are geometrically distributed is used in the sequel. This approximation method is efficient but two limitations must be mentioned:

- the resulting transfer function behaves exactly as a limited frequency band fractional integration operator with an infinite number of poles and zeros (Oustaloup et al., 2000) but becomes sub-optimal for a limited number of poles and zeros (Sabatier, 2018);
- the geometric distribution of poles and zeros is a particular case, as an infinite number of distributions is possible.

The latter limitation is demonstrated in this paper on the integral form of the impulse response of a fractional integrator. This integral form also permits a direct approximation with a Foster network with resistors and capacitors whose values are linked with defined functions.

For a geometric distribution for the resistor and capacitor values, it is also demonstrated in the paper that a Cauer network impedance also exhibits a power law type behaviour. From this geometric distribution, it is then shown that an infinity of other distributions is permitted to produce a power law type behaviour in the case of a Cauer network, reducing the geometric distribution to a particular case.

As a Cauer network can be viewed as the discrete form of a diffusion equation, the last part of the paper deduces diffusion equations with spatially variable coefficients that enable power law type behaviours to be produced. It is argued that this class of equations is a possible alternative to fractional diffusion equations for anomalous diffusion process modelling.

The main contributions of this paper are found in sections 3 to 6. Section 2 is dedicated to reminders on the approximation of a fractional order integrator and to the resulting electrical networks, results which will be used in the sequel of the paper. As a first contribution, section 3 shows that a geometric distribution of poles and zeros for the approximation of a fractional order integrator is only a particular distribution and that an infinity of other distributions are permitted. The analytic way to obtain these new distributions had never been presented before in the literature. Due to the close link between the approximations obtained and Foster type networks, section 3 also demonstrates as a new contribution that an infinity of Foster type networks can be used to produce power law type behaviours. Section 4 is dedicated to Cauer type networks. It is well known that a geometric distribution of the parameters in these networks produces power law type behaviours. But the present work proposes an analytical proof never published and uses it to produce other distributions (an infinity exist) of parameters that also lead to the same kind of behaviour. As a Cauer type network can be obtained through the discretisation of a heat equation, section 5 proposes a class of heat equation with spatially varying coefficients that produce power law type behaviours. This is another contribution of the paper that can be viewed as an alternative solution to fractional diffusion equation for anomalous diffusion modelling, without the limitations and drawbacks associated to fractional differentiation. The paper ends with a discussion and propositions for finding other spatially varying coefficients for the heat equation leading to power law type long memory behaviours.

2 – Prior art on the approximation of fractional order integrators and the resulting electrical networks

Fractional models and consequently fractional order integrator are infinite dimensional, thus their simulations or their implementations require their approximations. Many methods were proposed in the literature to obtain approximate models and many have overlaps so that it is not easy to categorize them. 28 methods are analysed in (Valerio and Sá da Costa, 2005). Some of them are implemented in digital tools, a comparison of which is proposed in (Li et al, 2017). Note also that discussions about power law in electrical circuits and some power-law relations in Laplace transforms can be found in (Tenreiro Machado et al, 2004) (Valério et al, 2013) (De Oliveira et al, 2014).

In most of these methods the fractional model is replaced by a classical integer model under various forms: continuous time model, discrete time model, electrical network (it is often simple to go from one form to another). Some apply to the full fractional model such as frequency domain fitting based methods (Bingi, 2019). But, as a fractional integrator chain appears in a fractional model, a large part of the proposed methods concentrates on the approximation of the fractional integrator of transfer function $s^{-\nu}$. Among all these methods, the following are the most common

- power series expansion (PSE) techniques based on Taylor series, Maclaurin series, etc. (Valério et al., 2013) (Petráš 2011) (Caponetto, 2010)
- continued fractional expansion based methods (Vinagre et al 2000),
- impulse response based method (Sabatier et al, 2016)
- time moments based approaches (Khanra et al., 2013),
- Carlson method based approaches (Carlson and Halijak, 1964),
- optimisation based methods (Bourouba et al, 2018),

- frequency distribution mode approach (Manabe, 1961), (Ichise et al., 1971), (Oustaloup, 1983) (Raynaud and Zergaïnoh, 2000) (Charef, 2006) (Wei et al, 2019).

In this last class of method, a widely used is the one known in the literature as the Oustaloup method (Oustaloup et al., 2000) although a similar approach was proposed by Manabe (Manabe, 1961). This method, based on a geometric distribution of mode is widespread because it comes in the form of a simple algorithm, given below.

Algorithm 1 - *In the frequency band* $[\omega_l, \omega_h]$*, the limited frequency band fractional integrator of transfer function* $I_{Lb}^{\nu}(s)$ *defined in (4) can be approximated by the transfer function* $I_N^{\nu}(s)$

$$I_{Lb}^{\nu}(s) = C_0 \left(\frac{1+\frac{s}{\omega_h}}{1+\frac{s}{\omega_l}}\right)^{\nu} \approx I_N^{\nu}(s) = C'_0 \frac{\prod_{k=1}^{N}\left(1+\frac{s}{\omega'_k}\right)}{\prod_{k=1}^{N}\left(1+\frac{s}{\omega_k}\right)} \qquad C_0 = \left(\frac{\sqrt{1+\left(\frac{1}{\omega_h}\right)^2}}{\sqrt{1+\left(\frac{1}{\omega_l}\right)^2}}\right)^{-\nu} . \tag{4}$$

As shown in (Oustaloup et al., 2000), the corner frequencies ω_k *and* ω'_k *(respectively the poles and zeros of the transfer function* $I_N^{\nu}(s)$*) are geometrically distributed to obtain the required frequency behaviour:*

$$r = \left(\frac{\omega_h}{\omega_l}\right)^{\frac{1}{N}} \qquad \alpha = r^{\nu} \qquad \eta = r^{1-\nu} \tag{5}$$

$$\omega_1 = \eta^{1/2}\omega_l \qquad \omega'_1 = \alpha\omega_1 \qquad \omega'_{k+1} = r\omega'_k \qquad \omega_{k+1} = r\omega_k \qquad k \in [1..N]. \tag{6}$$

■

Remark 1 *- As shown in (Oustaloup et al., 2000) this algorithm is exact as* N *tends towards infinity:*

$$I_{Lb}^{\nu}(s) = C_0 \lim_{N\to\infty} \frac{\prod_{k=1}^{N}\left(1+\frac{s}{\omega'_k}\right)}{\prod_{k=1}^{N}\left(1+\frac{s}{\omega_k}\right)} \qquad \text{and thus} \qquad r \to 1, \tag{7}$$

but becomes sub-optimal (Sabatier 2018) with a finite number of corner frequencies ω_k *and* ω'_k*. In this case, the sub optimality relates to the absolute and relative error between* $I_{Lb}^{\nu}(s)$ *and* $I_N^{\nu}(s)$ *for a given* N*.*

■

Using fraction expansion, approximation (4) can be rewritten as:

$$I_N^{\nu}(s) = \sum_{k=1}^{N} \frac{R_k}{1+\frac{s}{\omega_k}}. \tag{8}$$

If it is assumed that the transfer function $I_N^{\nu}(s)$ links an input current $I(s)$ to an output voltage $U(s)$, then, from relation (8) the following relation holds:

$$U(s) = \sum_{k=1}^{N} U_k(s) \quad \text{with} \quad U_k(s) = \frac{R_k}{1+\frac{s}{\omega_k}}\, I(s). \tag{9}$$

The transfer function $I_N^{\nu}(s)$ can thus be represented by the electrical network of figure 1 by introducing parameters C_k such that $R_k C_k = \omega_k$. Corner frequencies ω_k are linked by the ratio r so that $\omega_{k+1} = r\omega_k$. For large values of N, figure 2 shows that the following relations also hold:

$$R_{k+1} \approx \alpha R_k \quad \text{with} \quad C_{k+1} \approx \eta C_k \tag{10}$$

and the transfer function $I_N^{\nu}(s)$ exhibits a power law behaviour.

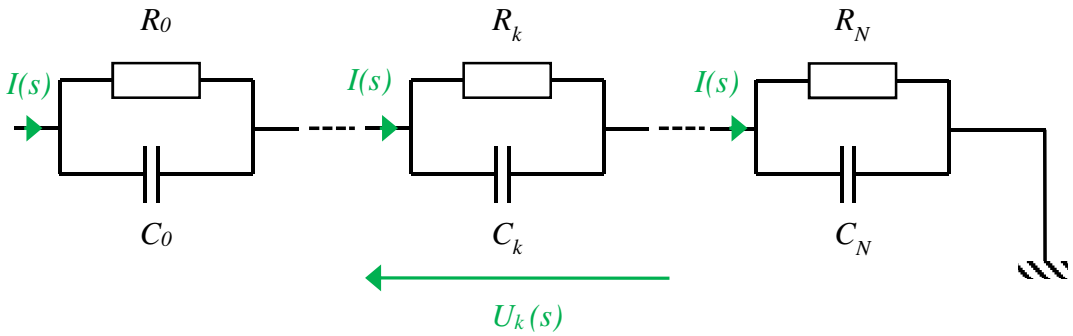

Figure 1 – *Electrical network (Foster type) whose impedance is* $I_N^{\nu}(s)$

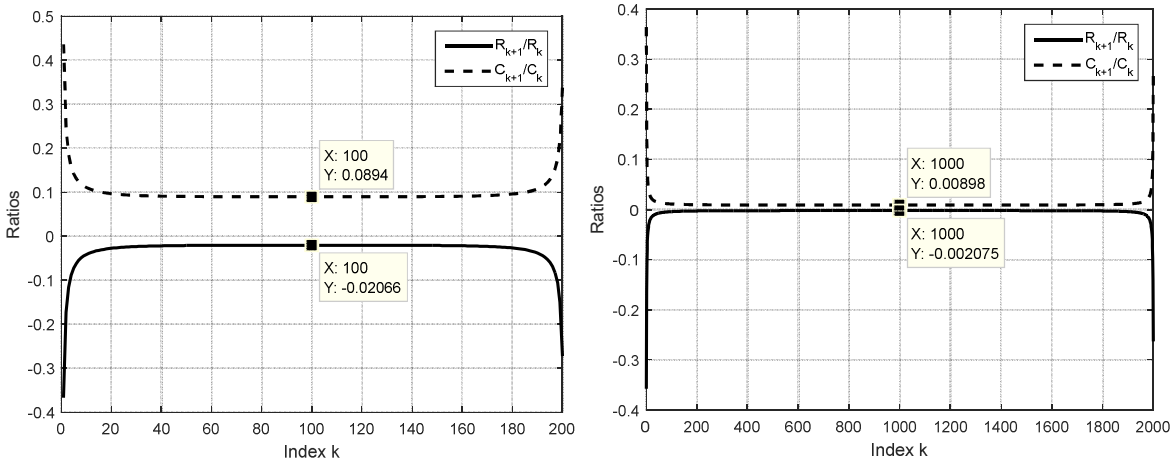

(a) (b)

Figure 2 – *Logarithm of ratios* $\frac{R_{k+1}}{R_k}$ *and* $\frac{C_{k+1}}{C_k}$ *in relation (10) for* $\omega_l = 1$, $\omega_h = 10^6$; $\nu = 0.3$ *with* $\alpha = 1.0208$, $\eta = 1.0493$ *and N= 200 (a) or* $\alpha = 1.0021$, $\eta = 1.0048$ *and N=2000 (b)*

This geometric distribution of corner frequencies or of components in the electrical network of figure 1 (electrical networks with resistors and inductors are also possible), now admitted by all, is however a particular case among an infinity of other possible distributions. Other distributions are presented in the next section: some can improve the optimality problem mentioned in remark 1 (Sabatier 2018), and can be applied to more complex transfer functions such as the one given by relation (4) (see appendix A.1).

3 – Beyond geometric distribution

Using the Cauchy method, the impulse response $h(t)$ of a fractional model of transfer function $H(s)$ can be written under the form

$$h(t) = \mathrm{L}^{-1}\{H(s)\} = \int_0^\infty \mu(x)\, e^{-tx} dx. \tag{11}$$

As an example, consider the transfer function

$$H(s) = \frac{1}{s^\nu}. \tag{12}$$

It can be shown that (Podlubny, 1999)

$$h(t) = \int_0^\infty \mu(x) e^{-tx}\, dx \qquad \text{with} \qquad \mu(x) = \frac{sin(\nu\pi)}{\pi x^\nu} \tag{13}$$

and thus

$$H(s) = \int_0^\infty \frac{\mu(x)}{s+x} dx. \tag{14}$$

Remark 2 *- If $h(t)$ is the impulse response of a model whose input is $u(t)$, the convolution product of relation (11) with an input $u(t)$ means that the model output can be written as:*

$$y(t) = \int_0^\infty \mu(x)\, w(t,x) dx, \qquad \dot{w}(t,x) = -xw(t,x) + u(t) \tag{15}$$

which is in fact the diffusive representation introduced by (Montseny, 1998) and (Matignon, 1998).

■

From the discretization of integral (14), it is easy to deduce an electrical network whose transfer function is an approximation of $H(s)$ on a given frequency range $[x_{min}, x_{max}]$. Using the Euler approximation method (but many other methods of higher order can be used), integral (14) can be approximated as follows:

$$H(s) = \int_0^\infty \frac{\mu(x)}{s+x} dx \approx H_a(s) = \sum_{k=0}^N \frac{\mu(x_k)\Delta x}{s+x_k}, \quad \text{with} \quad x_0 = x_{min} \tag{16}$$

with

$$x_0 = x_{min} \qquad \Delta x = \frac{x_{max} - x_{min}}{N} \qquad x_k = x_{min} + k\Delta x. \tag{17}$$

Applied to transfer function (12), the following approximation can be obtained

$$H(s) \approx H_a(s) = \frac{sin(\nu\pi)}{\pi} \sum_{k=0}^N \frac{x_k^{-\nu}}{s+x_k} \Delta x. \tag{18}$$

For $\nu = 0.4$, on the frequency range $[\omega_l, \omega_h]$ with $\omega_l = 0.001\, rd/s$ and $\omega_h = 1000$ rd/s the approximation $H_a(s)$ Bode diagrams are shown in figure 3 with several values

of N, ($N = 10^5$, $N = 5 * 10^5$, $N = 10^6$), showing that a large number N is required for the power law type behaviour appears.

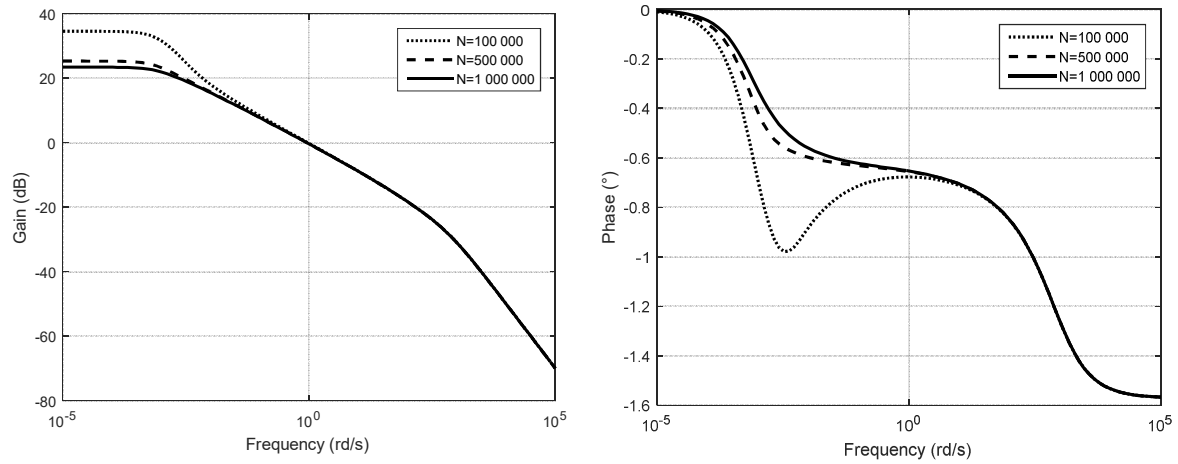

Figure 3 – *Bode diagram of $H_a(s)$ (given by relation (18))*

As relation (15) can be rewritten as

$$H_a(s) = \sum_{k=0}^{N} \frac{\frac{sin(\nu\pi)}{\pi} x_k^{-\nu-1}}{\frac{s}{x_k}+1} \Delta x \,, \tag{19}$$

it permits a realization using an RC network like the one in figure 1 with

$$R_k = \frac{sin(\nu\pi)}{\pi} x_k^{-\nu-1} \Delta x, \qquad C_k = \frac{1}{\frac{sin(\nu\pi)}{\pi} x_k^{-\nu-1} \Delta x} \quad \text{and} \quad \omega_k = \frac{1}{R_k C_k} = x_k \tag{20}$$

as the circuit impedance in figure 1 is

$$G(s) = \sum_{k=0}^{N} \frac{R_k}{R_k C_k s+1}. \tag{21}$$

Note that an RL (resistor-self) circuit can also be designed. Also note that this approximation method can be applied to many other transfer functions of which a non-exhaustive list is given in appendix A.1, table A.1. For instance, the impulse response of transfer function (4) is defined by (see appendix A.1)

$$\mathcal{L}^{-1}\left\{ I_a^{\nu}(s) = C_0 \frac{\left(\frac{s}{\omega_h}+1\right)^{\nu}}{\left(\frac{s}{\omega_l}+1\right)^{\nu}} \right\} = C_0 \left(\frac{\omega_l}{\omega_h}\right)^{\nu} \left(\delta(t) + \frac{sin(\nu\pi)}{\pi} \int_{\omega_b}^{\omega_h} \frac{(\omega_h - x)^{\nu}}{(x-\omega_l)^{\nu}(s+x)} dx \right) \tag{22}$$

where $\delta(t)$ is the Dirac impulse function. According to the previous comments,

$$I_{Lb}^{\nu}(s) \approx \mathrm{a}_0 + \sum_{k=0}^{N} \frac{\mathrm{a}_k}{\frac{s}{\omega_k}+1} \tag{23}$$

with

$$a_0 = C_0\left(\frac{\omega_l}{\omega_h}\right)^{\nu}, \qquad a_k = C_0\left(\frac{\omega_l}{\omega_h}\right)^{\nu} \frac{sin(\nu\pi)}{\pi} \frac{(\omega_h-\omega_k)^{\nu}}{(\omega_k-\omega_l)^{\nu}\omega_k} \Delta x, \tag{24}$$

$$\omega_k = \omega_h + k\Delta x, \qquad \Delta x = \frac{\omega_h-\omega_b}{N}.$$

Fraction expansion of $I_N^{\nu}(s)$ in relation (4) can also be written as

$$I_{Lb}^{\nu}(s) = a'_0 + \sum_{k=0}^{N} \frac{a'_k}{\frac{s}{\omega_k}+1}. \tag{25}$$

A comparison of coefficients a_k and a'_k is given by figure 4. It reveals that, for a large value of N, $a_k \approx a'_k$ and that the two approximations are very close.

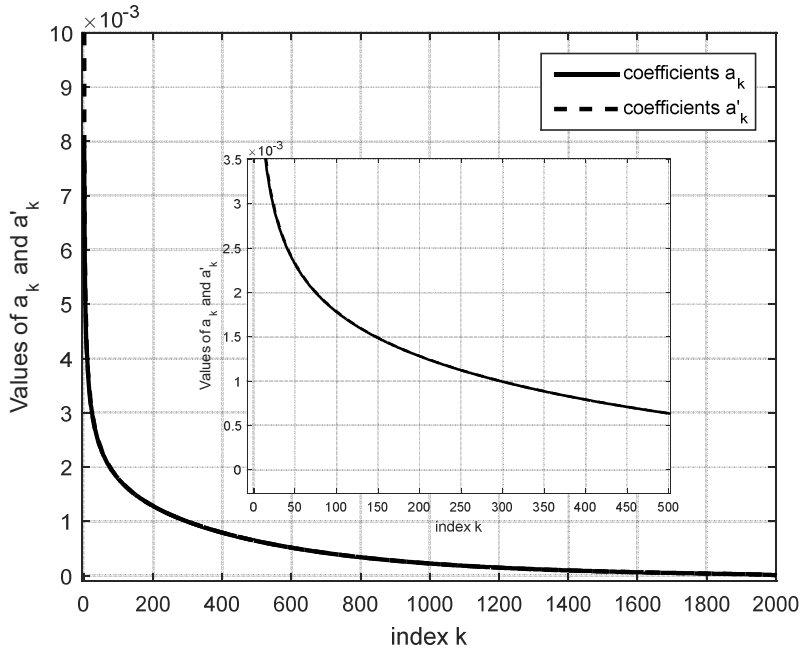

Figure 4 – *Comparison of coefficients* a_k and a'_k, with $N = 2000$ and $\nu = 0.3$, $\omega_l = 1\ rd/s$, $\omega_h = 10^6\ rd/s$ (zoom inside the figure)

If the transfer function $H(s)$ of relation (12) is considered again (for simplicity but a similar analysis can be done with the transfer functions of table A.1), relation (20) highlights that the capacitors and resistors are linked by the recurrence relations:

$$\frac{R_{k+1}}{R_k} = \frac{x_{k+1}^{-\nu-1}}{x_k^{-\nu-1}} \qquad \frac{C_{k+1}}{C_k} = \frac{x_k^{-\nu-1}}{x_{k+1}^{-\nu-1}}. \tag{26}$$

It can be noticed, that unlike relation (10), the ratios linking two resistors or two capacitors are not constant and depend on k. This discretization can be viewed as an alternative solution to algorithm 1, but as parameter N must be very large to have an accurate approximation on a large frequency band, it requires a very large number of components in the network of figure 1. Such a defect is due to the fixed step discretization of integral (11).

To overcome this defect, it is possible to search for a change of variable that contracts the frequency domain, thus making the fixed step discretization more efficient.

As a first try, the following change of variable is used in relation (14):

$$x = a^z = e^{z ln(a)} \quad \text{with} \quad a \in \mathbb{R}_+^* \quad \text{thus} \quad dx = ln(a) e^{z ln(a)} dz. \tag{27}$$

$H(s)$ can be rewritten as:

$$H(s) = \int_{-\infty}^{\infty} \frac{\mu(e^{z ln(a)})}{s + e^{z ln(a)}} ln(a) e^{z ln(a)} dz = \int_{-\infty}^{\infty} ln(a) \frac{\mu(e^{z ln(a)})}{\frac{s}{e^{z ln(a)}} + 1} dz. \tag{28}$$

This transfer function can be approximated by:

$$H_a(s) = \sum_{k=0}^{N} ln(a) \frac{\mu(e^{z_k ln(a)})}{\frac{s}{e^{z_k ln(a)}} + 1} \Delta z \tag{29}$$

with

$$z_0 = \frac{ln(x_{min})}{ln(a)} \qquad \Delta x = \frac{\frac{ln(x_{max})}{ln(a)} - \frac{ln(x_{min})}{ln(a)}}{N} \qquad z_k = \frac{ln(x_{min})}{ln(a)} + k\Delta z. \tag{30}$$

Such a discretisation permits the realization of figure 1 with:

$$R_k = \frac{sin(\nu\pi)}{\pi} ln(a) e^{-\nu z_k ln(a)} \Delta z \qquad C_k = \frac{1}{\frac{sin(\nu\pi)}{\pi} ln(a) e^{(-\nu+1) z_k ln(a)} \Delta z} \tag{31}$$

and

$$\omega_k = \frac{1}{R_k C_k} = e^{z_k ln(a)}\,. \tag{32}$$

If $= 0.4,\ a = 10, N = 10,\ \omega_l = 0.001\ rd/s,\ \omega_h = 1000$ rd/s, the Bode diagrams of the approximation $H_a(s)$ in relation (29) with change of variable (27) are shown in figure 5. They are very similar to those of figure 3 obtained with relation (18) and $N = 10^6$, thus showing the interest of the change of variable (27) in reducing the size of the approximation.

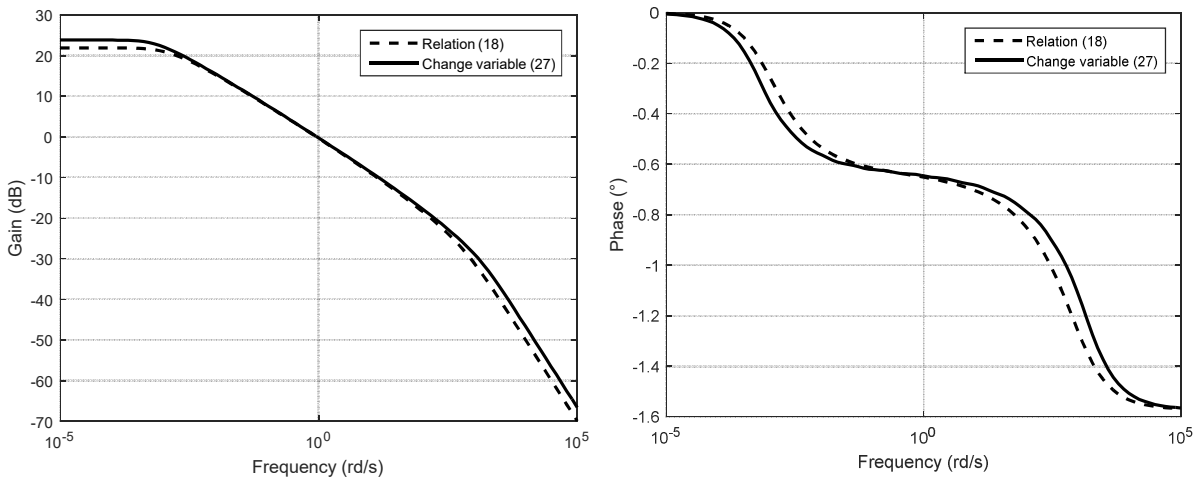

Figure 5 – *Bode diagram of $H_a(s)$ with change of variable (27) and comparison with the Bode diagrams of approximation (18)*

Remark 3*: Whatever the value of a, and as:*

$$z_{k+1} - z_k = \frac{ln(x_{min})}{ln(a)} + (k+1)\Delta z - \frac{ln(x_{min})}{ln(a)} - k\Delta z = \Delta z \tag{33}$$

it can be noticed that

$$\frac{R_{k+1}}{R_k} = \frac{e^{-\nu z_{k+1} ln(a)}}{e^{-\nu z_k ln(a)}} = e^{-\nu \Delta z ln(a)} \qquad \frac{C_{k+1}}{C_k} = \frac{1e^{(-\nu+1) z_{k+1} ln(a)}}{e^{(-\nu+1) z_k ln(a)}} = e^{(-\nu+1) ln(a)} \tag{34}$$

and

$$\frac{\omega_{k+1}}{\omega_k} = \frac{1}{R_k C_k} = e^{\Delta ln(a)}. \tag{35}$$

■

The previous relation highlights a geometric distribution of the values of resistors, capacitors and corner frequencies, defined by the following ratios:

$$\alpha = e^{-\nu \Delta z ln(a)} \qquad \eta = e^{(-\nu+1) ln(a)} \quad . \tag{36}$$

This geometric distribution generalises the one introduced by Oustaloup (Oustaloup, 1983) (Oustaloup et al., 2000). The latter is indeed a particular case obtained with $a = 10$, among the infinite number of distributions obtained for all the other values of a, and for other changes of variable that can be proposed instead of relation (27). Among this infinity, the following one is interesting as it also makes it possible to contract the frequency domain.

Using the following change of variable

$$z^n = x \quad \text{or} \quad z = x^{1/n} \quad \text{with} \quad n \in \mathbb{N}^* \quad \text{thus} \quad dx = nz^{n-1}dz \tag{37}$$

relation (14) can be rewritten as:

$$H(s) = \frac{sin(\nu\pi)}{\pi} \int_0^\infty \frac{z^{-\nu n}}{s+z^n} n z^{n-1} dz = \frac{sin(\nu\pi)}{\pi} \int_0^\infty n \frac{z^{-\nu n-1}}{\frac{s}{z^n}+1} dz \tag{38}$$

and permits the network of figure 1 with:

$$R_k = \frac{sin(\nu\pi)}{\pi} n z_k^{-\nu n-1} \Delta z, \qquad C_k = \frac{1}{\frac{sin(\nu\pi)}{\pi} n z_k^{-\nu n-1+n} \Delta z}, \tag{39}$$

and

$$\omega_k = \frac{1}{R_k C_k} = z_k^n \, . \tag{40}$$

If $\nu = 0.4,\ n = 60, N = 10, \omega_l = 0.001\ rd/s, \omega_h = 1000$ rd/s the Bode diagrams of the approximation $H_a(s)$ obtained by discretisation of integral (38) and change of variable (37) are shown in figure 6. They are compared with the Bode diagrams obtained with change of variable (27). The comparison reveals that the two changes of variable are of equivalent quality with the same complexity ($N = 10$).

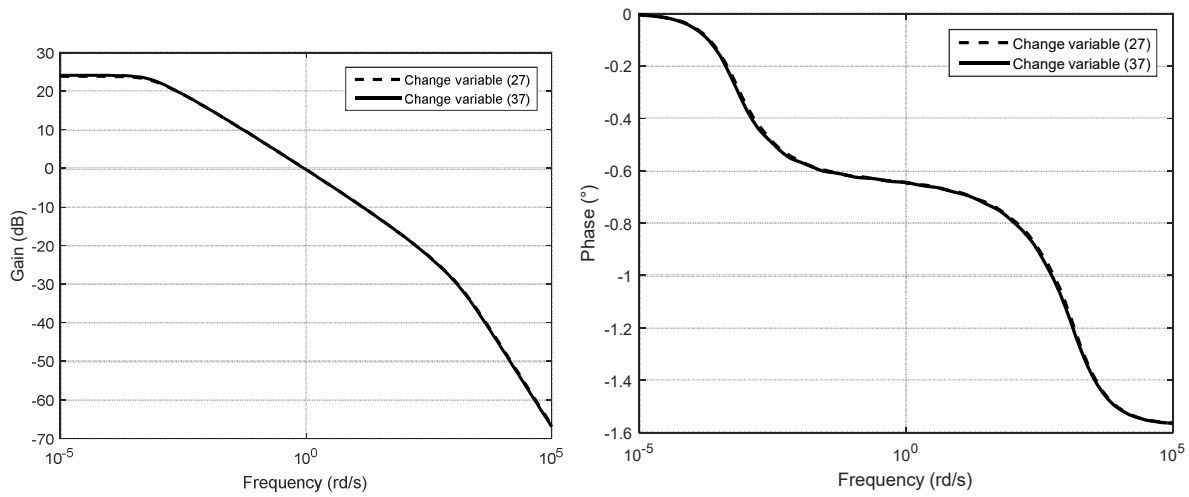

Figure 6 – *Bode diagram of $H_a(s)$ with the change of variable (37) and comparison with change of variable (27)*

As an infinity of changes of variable can be proposed, an infinity of Foster type networks can be used to generate a power law behaviour. The following section shows that Cauer networks can also generate this type of behaviour with an infinity of different distributions.

4 – Extension to Cauer type networks

The Cauer network of figure 7 is considered.

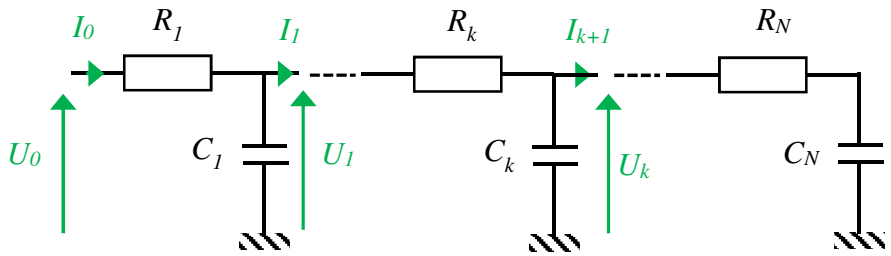

Figure 7 – Cauer type RC network

For the geometric distribution, such as the one defined by relations (5) and (6), an analytical result can be obtained to show that a Cauer type network generates a power law behaviour. Considering the network in figure 7, the following relations hold

$$\frac{1}{sC_k}\left(I_{k-1}(s) - I_k(s)\right) = U_k(s) \tag{41}$$

and

$$U_{k+1}(s) - U_k(s) = -R_k U_k(s). \tag{42}$$

From relations (41) and (42) respectively, it can be written that

$$\frac{U_k(s)}{U_{k-1}(s)} = \frac{\frac{1}{sC_k}}{1+\frac{1}{sC_k}\frac{I_k(s)}{U_k(s)}} \tag{43}$$

and

$$\frac{I_k(s)}{U_k(s)} = \frac{\frac{1}{R_k}}{1+\frac{1}{R_k}\frac{U_{i+1}(s)}{I_i(s)}}. \tag{44}$$

Combining relations (43) and (44), it can be shown that the input admittance of the network in figure 7 is defined by the continued fraction:

$$H(s) = \frac{I_0(s)}{U_0(s)} = \cfrac{\frac{1}{R_1}}{1+\cfrac{\frac{1}{sC_1R_1}}{1+\cfrac{\frac{1}{sC_1R_2}}{1+\cfrac{\frac{1}{sC_2R_2}}{1+\cdots}}}}. \tag{45}$$

Suppose that in figure 7, the resistors and capacitors are geometrically distributed and linked by the following ratios (as in (Oustaloup, 1983)):

$$\frac{R_{k+1}}{R_k} = \sigma \qquad \text{and} \qquad \frac{C_{k+1}}{C_k} = \rho, \tag{46}$$

and if $Z(s) = \frac{1}{sC_1R_1}$ relation (45) becomes

$$H(s) = \frac{I_0(s)}{U_0(s)} = \cfrac{\frac{1}{R_1}}{1+\cfrac{Z(s)}{1+\cfrac{Z(s)/\sigma}{1+\cfrac{Z(s)/\sigma\rho}{1+\cfrac{Z(s)/\sigma^2\rho}{1+\cfrac{Z(s)/\sigma^2\rho^2}{1+\cdots\cfrac{Z(s)/\sigma^N\rho^N}{1+Z(s)/\sigma^{N+1}\rho^N}}}}}}}. \tag{47}$$

Introducing the function

$$g(Z(s),\sigma,\rho) = \cfrac{Z(s)}{1+\cfrac{Z(s)/\sigma}{1+\cfrac{Z(s)/\sigma\rho}{1+\cfrac{Z(s)/\sigma^2\rho}{1+\cfrac{Z(s)/\sigma^2\rho^2}{1+\cdots\cfrac{Z(s)/\sigma^N\rho^N}{1+Z(s)/\sigma^{N+1}\rho^N}}}}}} \tag{48}$$

relation (48) becomes

$$H(s) = \frac{I_0(s)}{U_0(s)} = \frac{\frac{1}{R_1}}{1+g(Z(s),\sigma,\rho)}\,. \tag{49}$$

If N tends towards infinity, function $g(Z(s),\sigma,\rho)$ meets the following property:

Property 1 *– Function* $g(Z(s),\sigma,\rho)$ *meets the following relation* $g(Z(s),\sigma,\rho) = \frac{Z(s)}{1+g(Z(s),\rho,\sigma)}$

■

Thanks to property 1, the function $g(Z(s),\sigma,\rho)$ can be written under the form of a rational function with descending powers.

Theorem 1 *– With* $N \to \infty$

$$g(Z(s),\sigma,\rho) = \mathrm{K}(\sigma,\rho)Z(s)^{\nu}\left[\frac{1+\sum_{k=1}^{\infty} C_{2k-1}(\sigma,\rho)\left(\frac{Z(s)}{\sigma}\right)^{-\nu-k+1} + C_{2k}(\sigma,\rho)\left(\frac{Z(s)}{\sigma}\right)^{-k}}{1+\sum_{k=1}^{\infty} C_{2k-1}(\rho,\sigma)\left(Z(s)\right)^{-\nu-k+1} + C_{2k}(\rho,\sigma)\left(Z(s)\right)^{-k}}\right] \tag{50}$$

■

Using theorem 1, demonstrated in appendix A.2, for $|Z(s)| \gg 1$, (as $\sigma > 1$), admittance $H(s)$ meets the relation

$$H(s) \approx \frac{\frac{1}{R_1}}{K(\sigma,\rho)Z(s)^{\nu}}. \tag{51}$$

If the network results from an infinitesimal slicing of a continuous medium of abscissa z, the ratio of two consecutive components (capacitor or resistor) denoted F is given by :

$$\frac{F_{k+1}}{F_k} = \frac{F(kdz+dz)dz}{F(kdz)dz} \tag{52}$$

where dz denotes the thickness of the considered slices, with $dz \to 0$.

Given that

$$\frac{F(kdz+dz)-F(kdz)}{dz} = F'(kdz) \qquad dz \to 0 \tag{53}$$

where $F'(z)$ denotes the derivative of $F(z)$ and thus

$$F(kdz+dz) = F(kdz) + F'(kdz)dz \tag{54}$$

the ratio of relation (52) becomes

$$\frac{F_{k+1}}{F_k} = 1 + \frac{F\prime(kdz)}{F(kdz)}dz\,. \tag{55}$$

If this ratio, only a function of dz, is assumed constant $\forall k$ as in relation (46) and equal to Λ, using relation (55),

$$\Lambda = 1 + \frac{F\prime(kdz)}{F(kdz)}dz = 1 + \lambda_f dz \tag{56}$$

with

$$\frac{F\prime(kdz)}{F(kdz)} = \lambda_f. \tag{57}$$

After resolution of the differential equation (57), function $F(kdz)$ is given by

$$F(kdz) = F_0 e^{\lambda_f kdz} \qquad z \in [0, \infty[\,. \tag{58}$$

This shows that the lineic characteristics of the discretized medium that produces the network of figure 7 are defined by:

$$R(z) = R_0 e^{\lambda_R z} \qquad \text{and} \qquad C(z) = C_0 e^{\lambda_C z} \qquad z \in [0, \infty[. \tag{59}$$

The ratio of two consecutive resistors and capacitors is thus defined by:

$$\frac{R_{k+1}}{R_k} = \frac{R\big((k+1)dx\big)}{R(kdx)} = e^{\lambda_R \Delta z} \quad \text{and} \quad \frac{C_{k+1}}{C_k} = \frac{C\big((k+1)dx\big)}{C(kdx)} = e^{\lambda_C \Delta z}. \tag{60}$$

Now consider the change of variable $z = \log(x)$, $x \in [1, \infty[$, then relation (59) becomes

$$R(x) = R_0 x^{\lambda_R} \qquad \text{and} \qquad C(x) = C_0 x^{\lambda_C} \qquad x \in [1, \infty[. \tag{61}$$

With an infinitesimal slicing of the continuous medium, the system can be characterised by the network of figure 7 with:

$$R_k = R(kdx) = R_0 (kdx)^{\lambda_R} dx \qquad \text{and} \qquad C_k = C(kdx) = C_0 (kdx)^{\lambda_C} dx. \tag{62}$$

The ratio of two consecutive resistors and capacitors is thus defined by:

$$\frac{R_{k+1}}{R_k} = \frac{R_0\big((k+1)dx\big)^{\lambda_R} dx}{R_0 (kdx)^{\lambda_R} dx} = \frac{(k+1)^{\lambda_R}}{(k)^{\lambda_R}} \qquad \text{and} \qquad \frac{C_{k+1}}{C_k} = \frac{C_0\big((k+1)dx\big)^{\lambda_C} dx}{C_0 (kdx)^{\lambda_C} dx} = \frac{(k+1)^{\lambda_C}}{(k)^{\lambda_C}}. \tag{63}$$

These ratios are similar to those given by relation (26) for the Foster circuit of figure 1.

The following change of variable $z = \log(x^n)$, $x \in [1, \infty[$, $n \in \mathbb{N}_+^*$ is now considered. Relation (62) thus becomes

$$R(x) = R_0 x^{n\lambda_R} \qquad \text{and} \qquad C(x) = C_0 x^{n\lambda_C} \qquad x \in [1, \infty[. \tag{64}$$

With an infinitesimal slicing of the continuous medium, the system can be characterised by the network of figure 7 with:

$$R_k = R(kdx) = R_0(kdx)^{n\lambda_R}dx \qquad \text{and} \qquad C_k = C(kdx) = C_0(kdx)^{n\lambda_C}dx. \tag{65}$$

The ratio of two consecutive resistors and capacitors is thus defined by:

$$\frac{R_{k+1}}{R_k} = \frac{R_0\big((k+1)dx\big)^{n\lambda_R}dx}{R_0(kdx)^{n\lambda_R}dx} = \frac{(k+1)^{n\lambda_R}}{(k)^{n\lambda_R}} \qquad \text{and} \qquad \frac{C_{k+1}}{C_k} = \frac{C_0\big((k+1)dx\big)^{n\lambda_C}dx}{C_0(kdx)^{n\lambda_C}dx} = \frac{(k+1)^{n\lambda_C}}{(k)^{n\lambda_C}}. \tag{66}$$

These ratios are similar to those given by relation (39) for the Foster circuit of figure 1.

These networks and the associated distributions are used in the next section to introduce a class of heat equation that exhibits a power law type long memory behaviour.

5 – Heat equation with spatially variable coefficients for power law type long memory behaviour modelling

The following heat equation with spatially dependent parameters is now considered.

$$\frac{\partial T(z,t)}{\partial t} = \gamma(z)\frac{\partial}{\partial z}\left(\beta(z)\frac{\partial T(z,t)}{\partial z}\right) \tag{67}$$

with $z \in \mathbb{R}^+$.

This equation is a simplified form of the equation studied in [Levron et al. 1999]. Let

$$\varphi(z,t) = \beta(z)\frac{\partial T(z,t)}{\partial z}. \tag{68}$$

Discretisation of equation (68) with a discretisation step Δz leads to:

$$\varphi(z,t) = \beta(z)\frac{T(z+dz,t)-T(z,t)}{\Delta z} \tag{69}$$

and thus:

$$T(z,t) - T(z+dz,t) = -\frac{\Delta z}{\beta(z)}\varphi(z,t)\,. \tag{70}$$

Using relation (69), relation (67) can be rewritten as:

$$\frac{\partial T(z,t)}{\partial t} = \gamma(z)\frac{\partial \varphi(z,t)}{\partial z}\,. \tag{71}$$

Spatial discretisation of equation (71) with a discretisation step Δz leads to:

$$\frac{\partial T(z,t)}{\partial t} = \gamma(z)\frac{\varphi(z+dz,t)-\varphi(z,t)}{\Delta z} = \frac{\gamma(z)}{\Delta z}\big(\varphi(z+dz,t) - \varphi(z,t)\big)\,. \tag{72}$$

For $z = k\,\Delta z$ and if the following notations are introduced

$$C_k = -\frac{\Delta z}{\gamma(k\,\Delta z)} = C(k\,\Delta z\,)\Delta z \quad \text{and} \quad R_k = -\frac{\Delta z}{\beta(k\,\Delta z)} = R(k\,\Delta z\,)\Delta z \tag{73}$$

discretisation of equation (67) thus leads to the Cauer network of figure 8.

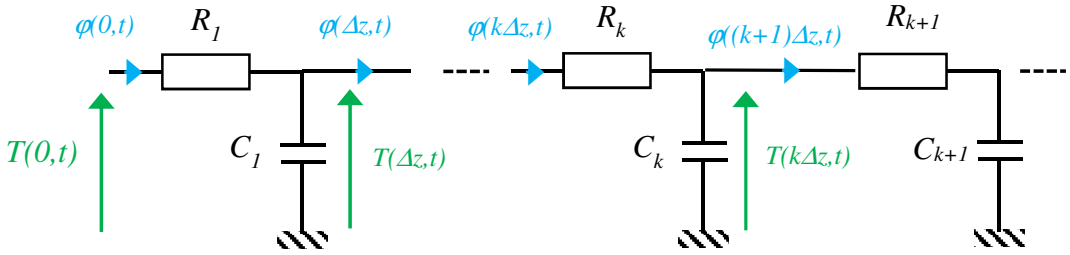

Figure 8 – Cauer type RC network resulting from the discretization of relation (67)

As $C_k = C(k\,\Delta z\,)\Delta z$ and $R_k = R(k\,\Delta z\,)\Delta z$, according to relations (46), (62) and (72), the transfer function $\varphi(0,s)/T(0,s)$ of the Cauer network of figure 8 exhibits a power law type long memory behaviour if

- $\frac{R_{k+1}}{R_k} = e^{\lambda_R \Delta z}$ and $\frac{C_{k+1}}{C_k} = e^{\lambda_C \Delta z}$ (relation (46)) (74)
- $\frac{R_{k+1}}{R_k} = \frac{(k+1)^{\lambda_R}}{(k)^{\lambda_R}}$ and $\frac{C_{k+1}}{C_k} = \frac{(k+1)^{\lambda_C}}{(k)^{\lambda_C}}$ (relation (62)) (75)
- $\frac{R_{k+1}}{R_k} = \frac{(k+1)^{n\lambda_R}}{(k)^{n\lambda_R}}$ and $\frac{C_{k+1}}{C_k} = \frac{(k+1)^{n\lambda_C}}{(k)^{n\lambda_C}}$ (relation (72)) (76)

and according to the relations (59), (60) and (63), the heat equation (67) exhibits a power law type long memory behaviour if (as $\gamma(z) = -1/C(z\,)$ and $\beta(z) = -1/R(z\,)$ according to relation (73))

- $\gamma(z) = -\frac{1}{C_0 e^{\lambda_C z}}$ and $\beta(z) = -\frac{1}{R_0 e^{\lambda_R z}}$ $z \in [0, \infty[$. (relation (59)) (77)
- $\gamma(z) = -\frac{1}{C_0 z^{\lambda_C}}$ and $\beta(z) = -\frac{1}{R_0 z^{\lambda_R}}$ $z \in [1, \infty[$ (relation (60)) (78)
- $\gamma(z) = -\frac{1}{C_0 z^{n\lambda_C}}$ and $\beta(z) = -\frac{1}{R_0 z^{n\lambda_R}}$ $z \in [1, \infty[$ (relation (63)) (79)

Of course, as previously explained, many other spatially varying coefficients can be obtained using other changes of variable than those proposed at the end of section 4.

6 – Discussions around some other distributions for further

Now, among the infinity of distributions that can be obtained using changes of variable as shown in section 3, the following is studied:

$$z = x^{-\nu}, \quad \text{or} \quad x = z^{-1/\nu} \quad \text{thus} \quad dx = -\frac{1}{\nu} z^{-\frac{1}{\nu}-1} dz. \tag{80}$$

Using this change of variable, relation (14) becomes:

$$H(s) = \frac{sin(\nu\pi)}{\pi}\int_{+\infty}^{0} \frac{z}{s+z^{-\frac{1}{\nu}}}\left(-\frac{1}{\nu}z^{-\frac{1}{\nu}-1}\right)dz = \frac{sin(\nu\pi)}{\pi}\int_{0}^{\infty}\frac{1}{\nu}\frac{z^{-\frac{1}{\nu}}}{s+z^{-\frac{1}{\nu}}}dz \tag{81}$$

or after simplification

$$H(s) = \frac{sin(\nu\pi)}{\nu\pi}\int_{0}^{\infty}\frac{1}{\frac{s}{z^{-\frac{1}{\nu}}}+1}dz \tag{82}$$

and permits the realization of figure 1 with:

$$H_a(s) = \sum_{k=0}^{N}\frac{R_k}{R_kC_ks+1} \qquad R_k = \frac{sin(\nu\pi)}{\nu\pi}\Delta z = Cte, \tag{83}$$

$$C_k = \frac{\nu\pi z_k^{\frac{1}{\nu}}}{\frac{sin(\nu\pi)}{\pi}\Delta z} \qquad \text{and} \qquad \omega_k = \frac{1}{R_kC_k} = z_k^{-\frac{1}{\nu}}.$$

If $= 0.4$, $N = 10000$, $\omega_l = 0.001\ rd/s$, $\omega_h = 1000\ rd/s$ the Bode diagrams of the approximation $H_a(s)$ are shown in figure 9. They are compared with the Bode diagrams of approximation (18) and the one obtained with change of variable (37). As for approximation (18), parameter N must be very large to have an accurate approximation of $s^{-\nu}$ on a large frequency band, but the interest of this change of variable is not there.

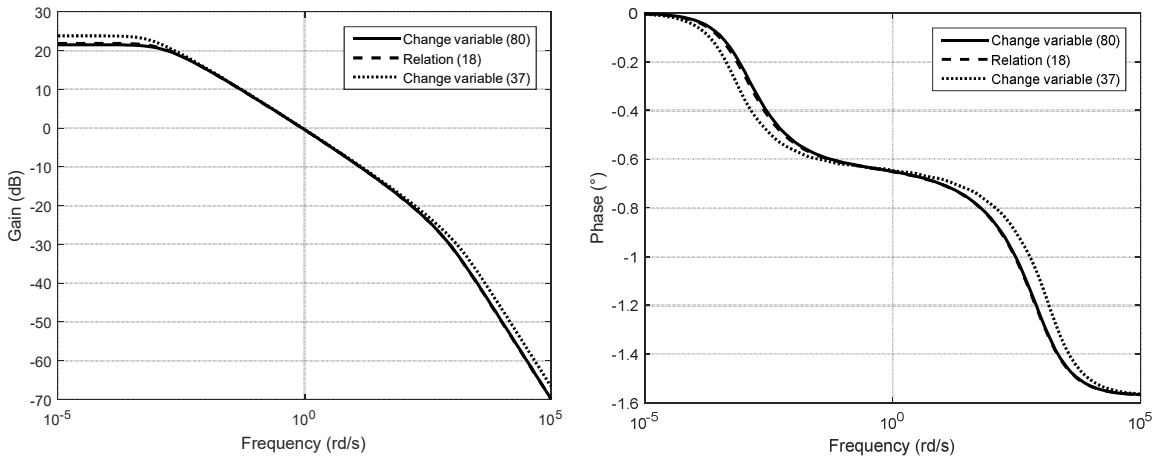

Figure 9 – *Bode diagram of $H_a(s)$ of relation (83) with change of variable (80) and comparisons with the Bode diagrams of approximation (18) and the one obtained with change of variable (37)*

The distribution of resistors and capacitors of relation (83) is now used to build the Cauer network of figure 7, with ν = 0.4, N=1000, $\Delta z = 2$ and

$$C_0 = \frac{\nu\pi}{\sin(\nu\pi)}. \tag{84}$$

The resulting Bode diagram of the transfer function $I_0(s)/U_0(s)$ is represented by figure 10. This diagram shows yet again that a power law behaviour can be obtained without a geometric distribution of resistors and capacitors. In this circuit, all the resistors have the same values and the capacitors are linked by the following relation

$$\frac{C_{k+1}}{C_k} = \frac{\left((N-k-1)\Delta z\right)^{\frac{1}{\nu}}}{\left((N-k)\Delta z\right)^{\frac{1}{\nu}}} = \frac{(N-k-1)^{\frac{1}{\nu}}}{(N-k)^{\frac{1}{\nu}}}. \tag{85}$$

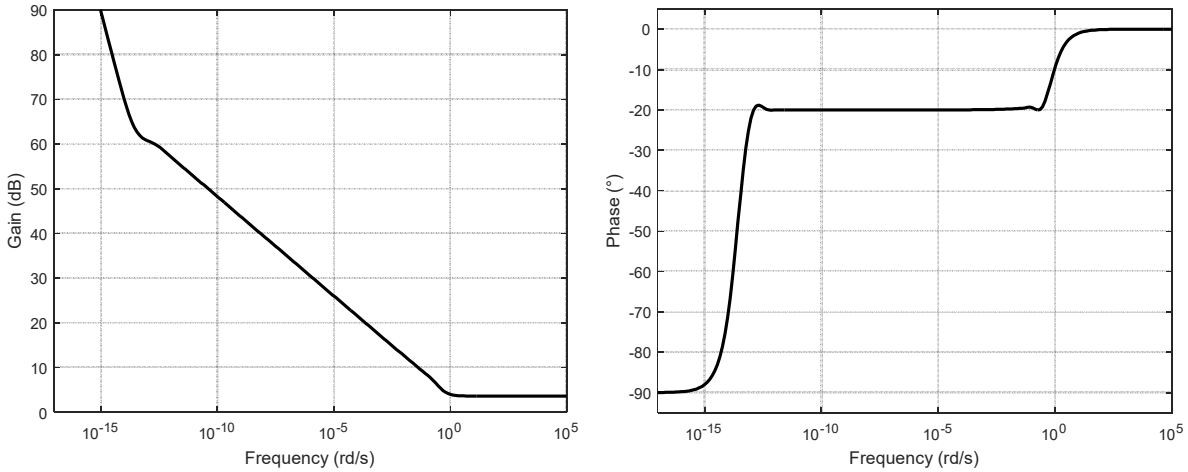

Figure 10 *– Bode diagram of transfer function $I_0(s)/U_0(s)$ of the Cauer type RC network with distribution of relation (83)*

This class of components distribution, that cannot be deduced using a change of variable in relation (59), and the resulting class of spatially varying coefficients in relation (67) will be studied by the author in future work.

7 – Conclusion

This paper shows that an infinity of

- pole and zero distributions (frequency modes) in classical integer transfer functions,

- passive component value distributions (such as capacitors or resistors) in Foster type networks,

can generate power law type long memory behaviours. Hence, the geometric distributions (Oustaloup 1983), (Oustaloup et al. 2000) often encountered in the literature are a particular case among an infinity of distributions.

For the Foster type network the proof is easy to establish using several changes of variables, as this network results directly from the discretisation of a filter transfer function that exhibits a power law behaviour. The proof for the Cauer type network is more tedious and is developed in the paper.

Due to the close link between Cauer type networks and heat equations (through discretisation), this paper also shows the ability of heat equations with a spatially variable coefficient to have a power law type long memory behaviour. This class of equation is thus another tool for power law type long memory behaviour modelling that solves the drawback

inherent in fractional heat equations. This class of equation will be more deeply studied by the author.

Finally, this paper shows, without proof, that other distributions and thus heat equations with spatially variable coefficients also exhibit power law type long memory behaviours. Moreover, by increasing the number of components in each branch of the Cauer network, it is possible to keep a power law behaviour, which suggests that there are a very large number of partial differential equations, other than the heat equations, which can produce a power law type long memory behaviour, some were already proposed in (Sabatier et al. 2013).

With reference to other papers recently published by the author (Sabatier, 2020.a) (Sabatier et al., 2020.c), this work is a new contribution to the dissemination of models not based on fractional differentiation but which exhibit power law type long memory behaviours.

Appendix 1 – Impulse response of some transfer functions that exhibit power law type long memory behaviours

The approximations given in section 3 are made on the integral form of the impulse response of the transfer function $H(s)=\frac{1}{s^{\nu}}$. The methodology used to derive the approximations and the change of variable used in sections 3 and 4 can be extended to other transfer functions. The following one is now considered:

$$H_1(s)=C_1\frac{\left(\frac{s}{\omega_h}+1\right)^{\nu-1}}{\left(\frac{s}{\omega_l}+1\right)^{\nu}} \qquad \text{with} \qquad C_1=\frac{\left(\left(\frac{1}{\omega_l}\right)^2+1\right)^{\frac{\nu}{2}}}{\left(\left(\frac{1}{\omega_h}\right)^2+1\right)^{\frac{\nu-1}{2}}}. \tag{A1.1}$$

The impulse response of $H_1(s)$ is defined by

$$h_1(t)=\frac{1}{2\pi j}\int_{c-j\infty}^{c+j\infty}H_1(s)e^{ts}ds \quad \text{with} \quad c>-\omega_l. \tag{A1.2}$$

For the computation of integral (A1.2), path $\Gamma=\gamma_0\cup\ldots\cup\gamma_7$ of figure A1.1 is considered with $c>-\omega_l$.

This path bypasses the negative axis around the branching point $z=-\omega_l$ and $z=-\omega_h$ for $t>0$. It thus avoids the complex plane domain for which the transfer function $H_1(s)$ is not defined, i.e. the segment $[-\omega_h,-\omega_l]$.

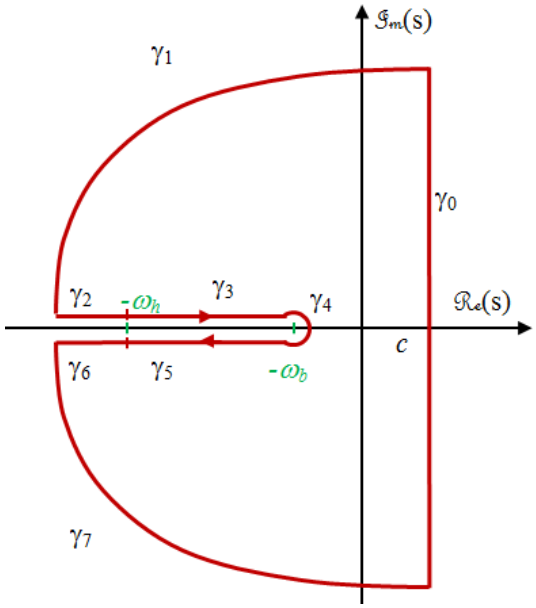

Figure A1.1 - *Integration path considered*

On path Γ, the radii of sub-path γ_1 and γ_7 tend towards infinity, and the radius of sub-path γ_4 tends towards 0. Using Cauchy's theorem with $c > -\omega_l$:

$$h_1(t) = \frac{1}{2\pi j}\int_{c-j\infty}^{c+j\infty} H_1(s)e^{ts}ds = -\frac{1}{2\pi j}\int_{\Gamma-\gamma_0} H_1(s)e^{ts}ds + \sum_{\substack{poles \\ in\,\Gamma}} \text{Res}[H_1(s)e^{ts}]. \tag{A1.3}$$

Since

$$\text{Res}[H_1(s)e^{ts}] = 0, \tag{A1.4}$$

operator $H_1(s)$ being strictly proper, by Jordan's lemma integrals on the large circular arcs of radius R, $R \to \infty$ can be neglected:

$$\int_{\gamma_1+\gamma_7} H_1(s)e^{ts}ds = 0. \tag{A1.5}$$

Let $s = xe^{j\pi}$, $x \in]\infty, \omega_h]$ on γ_2 and thus $ds = e^{j\pi}dx$. Let also $s = xe^{-j\pi}$, $x \in [\omega_h, \infty[$ on γ_6 and thus $ds = e^{-j\pi}dx$. Then

$$\int_{\gamma_2+\gamma_6} H_1(s)e^{ts}ds = \frac{{\omega_l}^\nu}{{\omega_h}^{\nu-1}}\int_{\infty}^{\omega_h} \frac{(xe^{j\pi}+\omega_h)^{\nu-1}}{(xe^{j\pi}+\omega_l)^\nu} e^{-xt}e^{j\pi}dx + \frac{{\omega_l}^\nu}{{\omega_h}^{\nu-1}}\int_{\omega_h}^{\infty} \frac{(xe^{-j\pi}+\omega_h)^{\nu-1}}{(xe^{-j\pi}+\omega_l)^\nu} e^{-xt}e^{-j\pi}dx = J_{\gamma_2+\gamma_6}(t) \tag{A1.6}$$

or

$$J_{\gamma_2+\gamma_6}(t) = \frac{{\omega_l}^{\nu}}{{\omega_h}^{\nu-1}} \int_{\infty}^{\omega_h} \frac{e^{j(\nu-1)\pi}(x-\omega_h)^{\nu-1}}{e^{j\nu\pi}(x-\omega_l)^{\nu}} e^{j\pi} e^{-xt} dx + \frac{{\omega_l}^{\nu}}{{\omega_h}^{\nu-1}} \int_{\omega_h}^{\infty} \frac{e^{-j(\nu-1)\pi}(x-\omega_h)^{\nu-1}}{e^{-j\nu\pi}(x-\omega_l)^{\nu}} e^{-j\pi} e^{-xt} dx \quad \text{(A1.7)}$$

and thus

$$J_{\gamma_2+\gamma_6}(t) = 0. \quad \text{(A1.8)}$$

Let $s = -\omega_l + \rho e^{j\theta}$, $\theta \in]-\pi, \pi]$ and thus $ds = j\rho e^{j\theta} d\theta$ with $\rho \to 0$, then

$$\int_{\gamma_4} H_1(s) e^{ts} ds = \frac{{\omega_l}^{\nu}}{{\omega_h}^{\nu-1}} \int_{\pi}^{-\pi} \frac{(-\omega_l+\omega_h+\rho e^{j\theta})^{\nu-1}}{(\rho e^{j\theta})^{\nu}} j\rho e^{j\theta} e^{t(-\omega_l+\rho e^{j\theta})} d\theta. \quad \text{(A1.9)}$$

As $\rho \to 0$

$$\int_{\gamma_4} I_{\nu}^{1}(s) e^{ts} ds = 0. \quad \text{(A1.10)}$$

Let $s = xe^{j\pi}$, $x \in [\omega_h, \omega_l]$ on γ_3 and thus $ds = e^{j\pi} dx$. Also let $s = xe^{-j\pi}$, $x \in [\omega_l, \omega_h]$ on γ_5 and thus $ds = e^{-j\pi} dx$. Then

$$\int_{\gamma_3+\gamma_5} H_1(s) e^{ts} ds = \frac{{\omega_l}^{\nu}}{{\omega_h}^{\nu-1}} \int_{\omega_h}^{\omega_l} \frac{\left(xe^{j\pi}+\omega_h\right)^{\nu-1}}{\left(xe^{j\pi}+\omega_l\right)^{\nu}} e^{-xt} e^{j\pi} dx + \frac{{\omega_b}^{\nu}}{{\omega_h}^{\nu-1}} \int_{\omega_l}^{\omega_h} \frac{(xe^{-j\pi}+\omega_h)^{\nu-1}}{(xe^{-j\pi}+\omega_l)^{\nu}} e^{-xt} e^{-j\pi} dx, \quad \text{(A1.11)}$$

and then

$$\int_{\gamma_3+\gamma_5} H_1(s) e^{ts} ds = \frac{{\omega_l}^{\nu}}{{\omega_h}^{\nu-1}} \int_{\omega_b}^{\omega_h} \frac{(\omega_h-x)^{\nu-1}}{(x-\omega_l)^{\nu}} (e^{j\nu\pi} - e^{-j\nu\pi}) e^{-xt} dx = 2j\sin(\nu\pi) \frac{{\omega_l}^{\nu}}{{\omega_h}^{\nu-1}} \int_{\omega_b}^{\omega_h} \frac{(\omega_h-x)^{\nu-1}}{(x-\omega_l)^{\nu}} e^{-xt} dx. \quad \text{(A1.12)}$$

As

$$h_1(t) = -\frac{1}{2\pi j} \int_{\Gamma-\gamma_0} H_1(s) e^{ts} ds \quad \text{(A1.13)}$$

using relations (A1.3), (A1.4), (A1.10) and (A1.12), the impulse response of $H_1(s)$ is given by, for $t > 0$:

$$h_1(t) = \frac{\sin(\nu\pi)}{\pi} \frac{{\omega_l}^{\nu}}{{\omega_h}^{\nu-1}} \int_{\omega_b}^{\omega_h} \frac{(\omega_h-x)^{\nu-1}}{(x-\omega_l)^{\nu}} e^{-xt} dx. \quad \text{(A1.14)}$$

The same calculation can be done, with other transfer functions, giving table A1.1.

$H_i(s)$	$h_{\mathrm{i}}(t)$
$\frac{\sum_{l=0}^{L} b_l s^{\beta_l}}{\sum_{k=0}^{K} a_k s^{\alpha_k}}$	$\sum_{i=1}^{r}\sum_{j=1}^{n_i} r_{ij} Y_j(t) e^{s_i t}$ $+\frac{1}{\pi}\int_0^{+\infty} \frac{\sum_{k=0}^{K}\sum_{l=0}^{L} a_k b_l \sin\big((\alpha_k-\beta_l)\pi\big) x^{\alpha_k+\beta_l}}{\sum_{k=0}^{K} a_k^2 x^{2\alpha_k} + \sum_{0\le k\le l\le K} a_k a_l \cos\big((\alpha_k-\alpha_l)\pi\big) x^{\alpha_k+\alpha_l}} e^{-xt} dx$ From (Matignon, 1998) with demonstration in (Sabatier et al., 2012). s_i are the poles.
$\frac{1}{s^{\nu}}$	$\frac{\sin(\nu\pi)}{\pi}\int_0^{+\infty} \frac{1}{x^{\nu}} e^{-xt} dx$
$\frac{1}{\left(\frac{s}{\omega_l}+1\right)^{\nu}}$	$\frac{\sin(\nu\pi)}{\pi}\int_{\omega_l}^{+\infty} \frac{{\omega_l}^{\nu}}{(x-\omega_l)^{\nu}} e^{-xt} dx$
$\frac{\left(\frac{s}{\omega_h}+1\right)^{\nu-1}}{\left(\frac{s}{\omega_l}+1\right)^{\nu}}$	$\frac{\sin(\nu\pi)}{\pi}\frac{{\omega_l}^{\nu}}{{\omega_h}^{\nu-1}}\int_{\omega_l}^{\omega_h} \frac{(\omega_h-x)^{\nu-1}}{(x-\omega_l)^{\nu}} e^{-xt} dx$
$\frac{\left(\frac{s}{\omega_h}+1\right)^{\nu}}{\left(\frac{s}{\omega_l}+1\right)^{\nu}}$	$(\frac{\omega_l}{\omega_h})^{\nu}\left(\delta(t)+\frac{sin(\nu\pi)}{\pi}\int_{\omega_b}^{\omega_h} \frac{(\omega_h-x)^{\nu}}{(x-\omega_l)^{\nu}(s+x)} dx\right)$ $\delta(t)$: Dirac impulse
$\frac{1}{s}\frac{\left(\frac{s}{\omega_l}+1\right)^{1-\nu}}{\left(\frac{s}{\omega_h}+1\right)^{1-\nu}}$	$\left(\frac{\omega_h}{\omega_l}\right)^{1-\nu}\left(H_e(t)+\frac{\sin\big((1-\nu)\pi\big)}{\pi}\int_{\omega_l}^{\omega_h} \frac{(x-\omega_l)^{1-\nu}}{x(\omega_h-x)^{1-\nu}} e^{-xt} dx\right)$ $H_e(t)$: Heaviside step function
$\frac{e^{-z\sqrt{as+b}}}{\sqrt{as+b}}$ $a>0,\ b>0,\ z>0$	$\frac{1}{\pi}\int_{\mathrm{b}/a}^{+\infty} \frac{\cos\big(z\sqrt{ax-b}\big)}{\sqrt{ax-b}} e^{-xt} dx$

Tab A1.1 – *Table of inverse Laplace transform of some transfer functions with power law type long memory behaviour*

Appendix 2 – Demonstration of theorem 1.

Suppose that the function $g(Z(s),\sigma,\rho)$ is given by:

$$g(Z(s),\sigma,\rho) = K(\sigma,\rho)Z(s)^{\nu(\sigma,\rho)}\left[\frac{1+\sum_{k=1}^{\infty} a_{2k-1}(\sigma,\rho)\big(Z(s)\big)^{-\nu(\sigma,\rho)-k+1}+a_{2k}(\sigma,\rho)\big(Z(s)\big)^{-k}}{1+\sum_{k=1}^{\infty} b_{2k-1}(\sigma,\rho)\big(Z(s)\big)^{-\nu(\rho,\sigma)-k+1}+b_{2k}(\sigma,\rho)\big(Z(s)\big)^{-k}}\right] \quad \text{(A2.1)}$$

where $0<\nu(\sigma,\rho)<1$ and $0<\nu(\rho,\sigma)<1$.

To make the demonstration easier to read, the following notations are used: ν, ν', K, a_k, b_k to denote respectively $\nu(\sigma,\rho)$, $\nu(\rho,\sigma)$, $K(\sigma,\rho)$, $a_k(\sigma,\rho)$, $b_k(\sigma,\rho)$. Relation (A2.1) can thus be rewritten:

$$g(Z(s),\sigma,\rho) = KZ(s)^{\nu}\left[\frac{1+\sum_{k=1}^{\infty} a_{2k-1}Z(s)^{-\nu-k+1}+a_{2k}Z(s)^{-k}}{1+\sum_{k=1}^{\infty} b_{2k-1}Z(s)^{-\nu'-k+1}+b_{2k}Z(s)^{-k}}\right]. \tag{A2.2}$$

Also, let K', a'_k, b'_k denote the functions $K(\rho,\sigma)$, $a_k(\rho,\sigma)$, $b_k(\rho,\sigma)$. The function $g(Z(s),\rho,\sigma)$ is thus defined by:

$$g(Z(s),\rho,\sigma) = K'Z(s)^{\nu'}\left[\frac{1+\sum_{k=1}^{\infty} a'_{2k-1}Z(s)^{-\nu'-k+1}+a'_{2k}Z(s)^{-k}}{1+\sum_{k=1}^{\infty} b'_{2k-1}Z(s)^{-\nu-k+1}+b'_{2k}Z(s)^{-k}}\right]. \tag{A2.3}$$

Now using $\mathcal{Z} = \frac{Z(s)}{\sigma}$, the function $g\left(\frac{Z(s)}{\sigma},\rho,\sigma\right)$ is defined by:

$$1 + g(\mathcal{Z},\rho,\sigma) = \frac{1+K'\mathcal{Z}^{\nu'}+\sum_{k=1}^{\infty} b'_{2k-1}\mathcal{Z}^{-\nu-k+1}+K'a'_{2k-1}\mathcal{Z}^{-k+1}+b'_{2k}\mathcal{Z}^{-k}+K'a'_{2k}\mathcal{Z}^{\nu'-k}}{1+\sum_{k=1}^{\infty} b'_{2k-1}\mathcal{Z}^{-\nu-k+1}+b'_{2k}\mathcal{Z}^{-k}} \tag{A2.4}$$

or

$$1 + g(\mathcal{Z},\rho,\sigma) = K'\mathcal{Z}^{\nu'}\frac{\left[1+\frac{\mathcal{Z}^{-\nu'}}{K'}+\sum_{k=1}^{\infty}\frac{b'_{2k-1}}{K'}\mathcal{Z}^{-\nu-\nu'-k+1}+a'_{2k-1}\mathcal{Z}^{-\nu'-k+1}+\frac{b'_{2k}}{K'}\mathcal{Z}^{-\nu'-k}+a'_{2k}\mathcal{Z}^{-k}\right]}{1+\sum_{k=1}^{\infty} b'_{2k-1}\mathcal{Z}^{-\nu-k+1}+b'_{2k}\mathcal{Z}^{-k}}$$

Taking into account property 1,

$$g(Z(s),\sigma,\rho) = \frac{Z(s)}{1+g(Z(s),\rho,\sigma)} \tag{A2.6}$$

and using relation (A2.5), the function $g(Z(s),\sigma,\rho)$ is given by:

$$g(Z(s),\sigma,\rho) = \frac{\sigma^{\nu'}Z(s)^{1-\sigma'}\left[1+\sum_{k=1}^{\infty} b'_{2k-1}Z(s)^{-\nu-k+1}+b'_{2k}Z(s)^{-k}\right]}{K'\left[1+\frac{Z(s)^{-\nu'}}{K'}+\sum_{k=1}^{\infty}\frac{b'_{2k-1}}{K'}Z(s)^{-\nu-\nu'-k+1}+a'_{2k-1}Z(s)^{-\nu'-k+1}+\frac{b'_{2k}}{K'}Z(s)^{-\nu'-k}+a'_{2k}Z(s)^{-k}\right]} \tag{A2.7}$$

Term-to-term identification of relations (A2.1) and (A2.7) leads to the following equations:

$$\nu + \nu' = 1 \qquad \text{or} \qquad \nu(\sigma,\rho) + \nu(\rho,\sigma) = 1 \tag{A2.8}$$

and

$$K = \frac{\sigma^{\nu'}}{K'} \qquad \text{or} \qquad K(\sigma,\rho)K(\rho,\sigma) = \sigma^{\nu(\rho,\sigma)}. \tag{A2.9}$$

Equation (A2.9) is symmetric in relation to ρ and σ. It is thus possible to write that

$$\sigma^{\nu(\rho,\sigma)} = K(\sigma,\rho)K(\rho,\sigma) = K(\rho,\sigma)K(\sigma,\rho) = \rho^{\nu(\sigma,\rho)} \tag{A2.10}$$

and thus

$$\sigma^{\nu(\rho,\sigma)} = \rho^{\nu(\sigma,\rho)} \tag{A2.11}$$

or taking the logarithm of relation (A2.10)

$$\nu(\rho,\sigma)log = \nu(\sigma,\rho)log(\rho). \tag{A2.12}$$

Using relation (A2.8), relation (A2.12) permits the following equations

$$\nu(\sigma,\rho) = \frac{log(\sigma)}{log(\sigma)+log(\rho)} \quad \text{and} \quad \nu(\rho,\sigma) = \frac{log(\rho)}{log(\sigma)+log(\rho)}. \tag{A2.13}$$

Term-to-term identification of relations (A2.1) and (A2.7) also permits the following equations:

$$a_{2k-1} = b'_{2k-1}\sigma^{\nu+k-1} \qquad \text{with} \qquad k \in \mathbb{N}^* \tag{A2.14}$$

$$b_{2k-1} = \left(a'_{2k-1} + \frac{b'_{2k-1}}{K'}\right)\sigma^{\nu'+k-1} \quad \text{with} \quad k \in \mathbb{N}^* \quad \text{and} \quad b'_0 = 1 \tag{A2.15}$$

$$a_{2k} = b'_{2k}\sigma^{k} \qquad \text{with} \qquad k \in \mathbb{N}^* \tag{A2.16}$$

$$b_{2k} = \left(a'_{2k} + \frac{b'_{2k-1}}{K'}\right)\sigma^{k} \quad \text{with} \quad k \in \mathbb{N}^*. \tag{A2.17}$$

Equation (A2.14) being symmetric in relation to ρ and σ, it can be rewritten as

$$a'_{2k-1} = b_{2k-1}\sigma^{\nu'+k-1} \qquad \text{with} \qquad k \in \mathbb{N}^* \tag{A2.18}$$

enabling equation (A2.15) to be rewritten as

$$b_{2k-1} = b_{2k-1}(\rho\sigma)^{\nu'+k-1} + \frac{b'_{2k-2}}{K'}\sigma^{\nu'+k-1} \quad \text{with} \quad k \in \mathbb{N}^* \quad \text{and} \quad b'_0 = 1 \tag{A2.19}$$

or using relation (A2.9):

$$b_{2k-1} = \frac{Kb'_{2k-2}\sigma^{k-1}}{\left(1-(\rho\sigma)^{\nu'+k-1}\right)} \quad \text{with} \quad k \in \mathbb{N}^* \quad \text{and} \quad b'_0 = 1. \tag{A2.20}$$

Equation (A2.20) being symmetric in relation to ρ and σ, it can be rewritten as

$$b'_{2k-1} = \frac{K'b_{2k-2}\rho^{k-1}}{\left(1-(\rho\sigma)^{\nu+k-1}\right)} \quad \text{with} \quad k \in \mathbb{N}^* \quad \text{and} \quad b_0 = 1. \tag{A2.21}$$

Also, equation (A2.16) being symmetric in relation to ρ and σ, it can be rewritten as

$$a'_{2k} = b_{2k}\rho^k \qquad \text{with} \qquad k \in \mathbb{N}^* \tag{A2.22}$$

enabling equation (A2.17) to be rewritten as

$$b_{2k} = b_{2k-1}(\rho\sigma)^k + \frac{b'_{2k-2}}{K\prime}\sigma^k \quad \text{with} \quad k \in \mathbb{N}^* \tag{A2.23}$$

and thus

$$b_{2k} = \frac{b_{2k-1}\sigma^k}{K\prime\left(1-(\rho\sigma)^k\right)} \quad \text{with} \quad k \in \mathbb{N}^* \quad \text{and} \quad b'_1 = \frac{K\prime}{1-\sigma} \tag{A2.24}$$

or given relation (A2.21)

$$b_{2k} = \frac{b_{2k-2}\sigma^k\rho^{k-1}}{\left(1-(\rho\sigma)^k\right)\left(1-(\rho\sigma)^{\nu+k-1}\right)} \quad \text{with} \quad k \in \mathbb{N}^* \quad \text{and} \quad b_0 = 1. \tag{A2.25}$$

The symmetric form of relation (A2.25) in relation to ρ and σ permits to write

$$b'_{2k} = \frac{b'_{2k-2}\rho^k\sigma^{k-1}}{\left(1-(\rho\sigma)^k\right)\left(1-(\rho\sigma)^{\nu\prime+k-1}\right)} \quad \text{with} \quad k \in \mathbb{N}^* \quad \text{and} \quad b'_0 = 1. \tag{A2.26}$$

The set of relations (A2.13), (A2.21) and (A2.25) thus prove that the function $g(Z(s),\sigma,\rho)$ meets the relation

$$g(Z(s),\sigma,\rho) = \mathrm{K}(\sigma,\rho)Z(s)^{\nu}\left[\frac{1+\sum_{k=1}^{\infty} C_{2k-1}(\rho,\sigma)\mathrm{K}(\rho,\sigma)\left(\frac{Z(s)}{\sigma}\right)^{-\nu-k+1} + C_{2k}(\rho,\sigma)\left(\frac{Z(s)}{\sigma}\right)^{-k}}{1+\sum_{k=1}^{\infty} C_{2k-1}(\sigma,\rho)\mathrm{K}(\sigma,\rho)\left(Z(s)\right)^{-\nu\prime-k+1} + C_{2k}(\sigma,\rho)\left(Z(s)\right)^{-k}}\right] \tag{A2.27}$$

with

$$\nu(\sigma,\rho) = \frac{log(\sigma)}{log(\sigma)+log(\rho)} \qquad 0 < \nu(\sigma,\rho) < 1 \tag{A2.28}$$

$$c_{2k}(\sigma,\rho) = \frac{\sigma^k\rho^{k-1}}{\left(1-(\rho\sigma)^k\right)\left(1-(\rho\sigma)^{\nu+k-1}\right)}\, c_{2k-2}(\sigma,\rho) \qquad k \in \mathbb{N}^* \quad \text{and} \quad c_0(\sigma,\rho) = 1 \tag{A2.29}$$

$$c_{2k-1}(\sigma,\rho) = \frac{\sigma^{k-1}}{\left(1-(\rho\sigma)^{\nu\prime+k-1}\right)} \quad \text{with} \quad k \in \mathbb{N}^* - \{1\} \quad \text{and} \quad c_1(\sigma,\rho) = \frac{1}{1-\rho}. \tag{A2.30}$$

In relation (A2.27), only coefficient $\mathrm{K}(\sigma,\rho)$ remains to be computed. It is possible to give an expression of $\mathrm{K}(\sigma,\rho)$ in the form of a ratio of two series as equation (A2.27) can be rewritten as:

$$g(Z(s),\sigma,\rho) = \mathrm{K}(\sigma,\rho)Z(s)^{\nu}\left[\frac{1+\mathrm{K}(\rho,\sigma)h_1\left(\frac{Z(s)}{\sigma},\rho,\sigma\right)+h_2\left(\frac{Z(s)}{\sigma},\rho,\sigma\right)}{1+\mathrm{K}(\sigma,\rho)h_1(Z(s),\sigma,\rho)+h_2(Z(s),\sigma,\rho)}\right] \tag{A2.31}$$

or using relation (A2.9)

$$g(Z(s),\sigma,\rho) = \mathrm{K}(\sigma,\rho)Z(s)^{\nu}\left[\frac{1+\frac{\sigma^{\nu}}{\mathrm{K}(\sigma,\rho)}h_1\left(\frac{Z(s)}{\sigma},\rho,\sigma\right)+h_2\left(\frac{Z(s)}{\sigma},\rho,\sigma\right)}{1+\mathrm{K}(\sigma,\rho)h_1(Z(s),\sigma,\rho)+h_2(Z(s),\sigma,\rho)}\right], \quad \text{(A2.32)}$$

with

$$h_1(Z(s),\sigma,\rho) = \sum_{k=1}^{\infty} C_{2k-1}(\sigma,\rho)Z(s)^{-\nu\prime-k+1}, \quad \text{(A2.33)}$$

and

$$h_2(Z(s),\sigma,\rho) = \sum_{k=1}^{\infty} C_{2k}(\sigma,\rho)Z(s)^{-k}. \quad \text{(A2.34)}$$

Now using $Z(s) = 1$ in relation (A2.32), coefficient $\mathrm{K}(\sigma,\rho)$ is given by:

$$\mathrm{K}(\sigma,\rho) = \left[\frac{g(1,\sigma,\rho)+h_2(1,\sigma,\rho)-\sigma^{\nu}h_1(1,\rho,\sigma)}{1-h_1(1,\sigma,\rho)+h_2(1,\rho,\sigma)}\right]. \quad \text{(A2.35)}$$

Conflicts of Interest: The authors declare no conflict of interest.

References

Bingi K., Ibrahim R., Karsiti M. N., Hassam S. M., Rajah V. (2019), Frequency Response Based Curve Fitting Approximation of Fractional–Order PID Controllers, International Journal of Applied Mathematics and Computer Science, Vol. 29, n°2, pp 311-326.

Bisquert J., Garcia-Belmonte G. (1997), Complex plane analysis of pn junction forward-voltage impedance, Electronics Letters, Vol. 33, n° 10, pp 900-901.

Bisquert J., Garcia-Belmonte G., Fabregat-Santiago F., Bueno P.R. (1999), Theoretical models for ac impedance of finite diffusion layers exhibiting low frequency dispersion, Journal of Electroanalytical Chemistry, Vol. 475, N° 2, pp 152-163.

Bisquert J., Compte A. (2001), Theory of the electrochemical impedance of anomalous diffusion, Journal of Electroanalytical Chemistry, Vol. 499, pp 112–120.

Bourouba B, Ladaci S, Chaabi A. (2018), Reduced-order model approximation of fractional-order systems using differential evolution algorithm. Journal of Control, Automation and Electrical Systems, Vol 29, N° 1, pp 32–43.

Caponetto, R. (2010), Fractional Order Systems: Modeling and Control Applications, World Scientific, Singapore.

Carlson G.E., Halijak C. A. (1964), Approximation of fractional capacitors (1/s)1/n by a regular Newton process. IEEE Trans. on Circuit Theory, 11 (2), 210–213.

Charef, A. (2006), Analogue realisation of fractional-order integrator, differentiator and fractional PI/^ lambda/D/^ mu/ controller. IEE Proc. Control Theory Appl., 153, 714–720.

De Oliveira E. C., Tenreiro Machado J. A. (2014), A Review of Definitions for Fractional Derivatives and Integral, Mathematical Problems in Engineering, Vol. 2014, Article ID 238459

Evangelista L. R., Lenzi E. K. (2018), Fractional Diffusion Equations and Anomalous Diffusion, Cambridge University Press.

Ichise M., Nagayanagi Y., Kojima T. (1971), An analog simulation of non-integer order transfer functions for analysis of electrode processes. J. Electroanal. Chem. Interfacial Electrochem., 33, 253–265.

M. Khanra M., Pal J., Biswas K. (2013), Rational Approximation and Analog Realization of Fractional Order Transfer Function with Multiple Fractional Powered Terms, Asian Journal of Control, Vol.15, N° 3, pp 723-735.

Levron F., Sabatier J., Oustaloup A., Habsieger L. (1999), From partial differential equations of propagative recursive systems to non integer differentiation - Fractional Calculus and Applied Analysis (FCAA): an international journal for theory and applications, Vol. 2, N° 3, pp. 246-264.
Li Z., Liu L., Dehghan S., Chen Y., Xue D. (2017), A review and evaluation of numerical tools for fractional calculus and fractional order controls, International Journal of Control, Vol. 90, N° 6.
Lindmayer J., Wrigley C. Y. (1965), Fundamentals of Semiconductor Devices, Van Nostrand, New York.
Manabe, S. (1961), The non-integer Integral and its Application to control systems. ETJ Jpn., 6, 83–87.
Matignon D. (1998), Stability properties for generalized fractional differential systems, ESAIM: Proc. 5, pp 145-158.
Montseny G. (1998), Diffusive representation of pseudo-differential time-operators, ESAIM: Proc. vol 5, pp 159-175.
Oustaloup, A. (1983), Systèmes Asservis Linéaires d'ordre Fractionnaire; Masson: Paris, France.
Oustaloup, A. Levron, F. Mathieu, B. Nanot, F. (2000), Frequency-band complex non integer differentiator: characterization and synthesis, IEEE Transactions on Circuits and Systems I: Fundamental Theory and Applications, Vol 47, N° 1, pp 25-39.
Petráš, I. (2011), Fractional derivatives, fractional integrals, and fractional differential equations in Matlab, in A. Assi(Ed.), Engineering Education and Research Using MATLAB, InTech, London, pp. 239–264.
Podlubny I. (1999), Fractional differential equations. Mathematics in Sciences and Engineering. Academic Press.
Randles J. E. B. (1947), Kinetics of rapid electrode reactions, Discussion of the Faraday Society, Vol. 1, pp 11-19.
Raynaud, H.F.; Zergaïnoh, A. (2000), State-space representation for fractional order controllers. Automatica, 36, 1017–1021.
Sabatier J., Merveillaut M., Malti R., Oustaloup A. (2010), How to Impose Physically Coherent Initial Conditions to a Fractional System?, Communications in Nonlinear Science and Numerical Simulation, Vol. 15, N° 5.
Sabatier J., Farges C., Merveillaut M., Feneteau L. (2012), On observability and pseudo state estimation of fractional order systems, European Journal of Control, n°3, pp 1-12.
Sabatier J., Nguyen H. C., Moreau X., Oustaloup A. (2013), Fractional behaviour of partial differential equations whose coefficients are exponential functions of the space variable, Mathematical and Computer Modelling of Dynamical Systems: Methods, Tools and Applications in Engineering and Related Sciences, Vol19, N°5.
Sabatier J., Farges C. and Trigeassou J. C. (2014), Fractional systems state space description: some wrong ideas and proposed solutions, Journal of vibration and control, Vol.20, N° 7, pp. 1076 – 1084, 2014.
Sabatier J., Farges C., Fadiga L. (2016), Approximation of a fractional order model by an integer order model: a new approach taking into account approximation error as an uncertainty, Journal on Vibration and Control, Vol. 22, n° 8, pp. 2069-2082.
Sabatier J., Farges C. (2018), Comments on the description and initialization of fractional partial differential equations using Riemann-Liouville's and Caputo's definitions, Journal of Computational and Applied Mathematics, Volume 339, pp 30-39.
Sabatier J. (2018), Solutions to the Sub-Optimality and Stability Issues of Recursive Pole and Zero Distribution Algorithms for the Approximation of Fractional Order Models, Algorithms, Vol 11, N° 7, p103.
Sabatier J., Rodriguez Cadavid S., Farges C. (2019), Advantages of limited frequency band fractional integration operator in fractional models definition, Conference on Control, Decision and Information Technologies, CoDIT 2019, Paris, France, April 23-26.
Sabatier J. (2020.a), Power Law Type Long Memory Behaviors Modeled with Distributed Time Delay Systems, Fractional and Fractals, Vol 4, n°1.
Sabatier J. (2020.b), Non-singular kernels for modelling power law type long memory behaviours and beyond, accepted for publication in Cybernetics.
Sabatier J., Farges C., Tartaglione V. (2020.c), Some alternative solutions to fractional models for modelling long memory behaviors, Mathematics, 8, 196; doi:10.3390/math8020196
Sluythers-Rehbach M., J.H. Sluythers J. H., in: E. Yeager, J.O.'M. Bockris, B.E. Conway, S. Sarangapani (Eds.) (1984), Comprehensive Treatise of Electrochemistry, vol. 9, Plenum Press, New York, 1984.
Tartaglione V., Farges C., Sabatier J. (2020), Dynamical modelling of random sequential adsorption, Paper proposed to the European Control Conference ECC 2020, St-Petersburg, Russia.
Tenreiro Machado J. A., Jesus I. S. (2004), A Suggestion from the Past?, Fractional Calculus and Applied Analysis, vol. 7, n. 4, pp. 403-407.
Valerio D., Sá da Costa J (2005), Time-domain implementation of fractional order controllers, IEE Proceedings - Control Theory and Applications, Vol. 152, N° 5, p 539.
Valério, D., Trujillo, J.J., Rivero, M., Machado, J.T., Baleanu, D. (2013), Fractional calculus: A survey of useful formulas, The European Physical Journal Special Topics, Vol 222, n°8, pp 1827-1846.

694 Van Herle J., McEvoy A. J. (1994), Oxygen diffusion through silver cathodes for solid oxide fuel cells, Journal
695 of Physics and Chemistry of Solids, Vol. 55, N° 4, pp 339-347,
696 Vetter K. J. (1967), Electrochemical Kinetics, Academic Press, New York.
697 Vinagre, B., Podlubny, I., Hernandez, A. and Feliu, V. (2000), Some approximations of fractional order
698 operators used in control theory and applications, Fractional Calculus and Applied Analysis Vol. 3, n°3, pp
699 231–248.
700 Warburg E. (1901), Ueber die Polarisationscapacität des Platins, Annalen der Physik, Vol. 311, n°9, pp 125-135.
701 Wei Y., Wang J., Liu T., Wang Y. (2019), Fixed pole based modeling and simulation schemes for fractional
702 order systems, ISA Transactions, Vol 84, pp 43-54.

Graphical Abstract

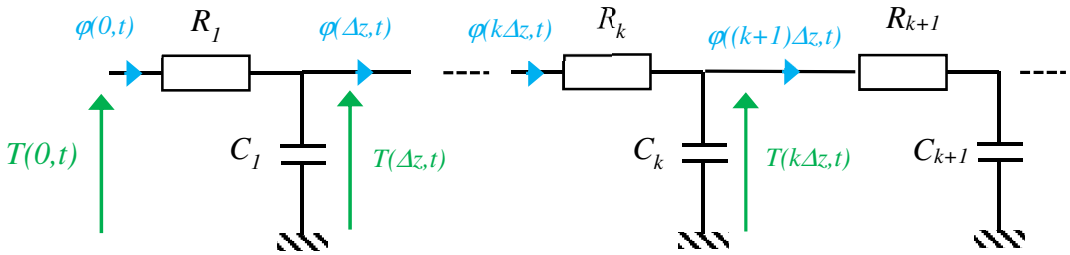

$$\frac{R_{k+1}}{R_k} = e^{\lambda_R \Delta z} \quad \text{and} \quad \frac{C_{k+1}}{C_k} = e^{\lambda_C \Delta z}$$

$$\frac{R_{k+1}}{R_k} = \frac{(k+1)^{\lambda_R}}{(k)^{\lambda_R}} \quad \text{and} \quad \frac{C_{k+1}}{C_k} = \frac{(k+1)^{\lambda_C}}{(k)^{\lambda_C}}$$

$$\frac{R_{k+1}}{R_k} = \frac{(k+1)^{n\lambda_R}}{(k)^{n\lambda_R}} \quad \text{and} \quad \frac{C_{k+1}}{C_k} = \frac{(k+1)^{n\lambda_C}}{(k)^{n\lambda_C}}$$

$$\frac{\partial T(z,t)}{\partial t} = \gamma(z)\frac{\partial}{\partial z}\left(\beta(z)\frac{\partial T(z,t)}{\partial z}\right) \qquad \varphi(z,t) = \beta(z)\frac{\partial T(z,t)}{\partial z}.$$

$$\gamma(z) = -\frac{1}{C_0 e^{\lambda_C z}} \quad \text{and} \quad \beta(z) = -\frac{1}{R_0 e^{\lambda_R z}}$$

$$\gamma(z) = -\frac{1}{C_0 z^{\lambda_C}} \quad \text{and} \quad \beta(z) = -\frac{1}{R_0 z^{\lambda_R}}$$

$$\gamma(z) = -\frac{1}{C_0 z^{n\lambda_C}} \quad \text{and} \quad \beta(z) = -\frac{1}{R_0 z^{n\lambda_R}}$$

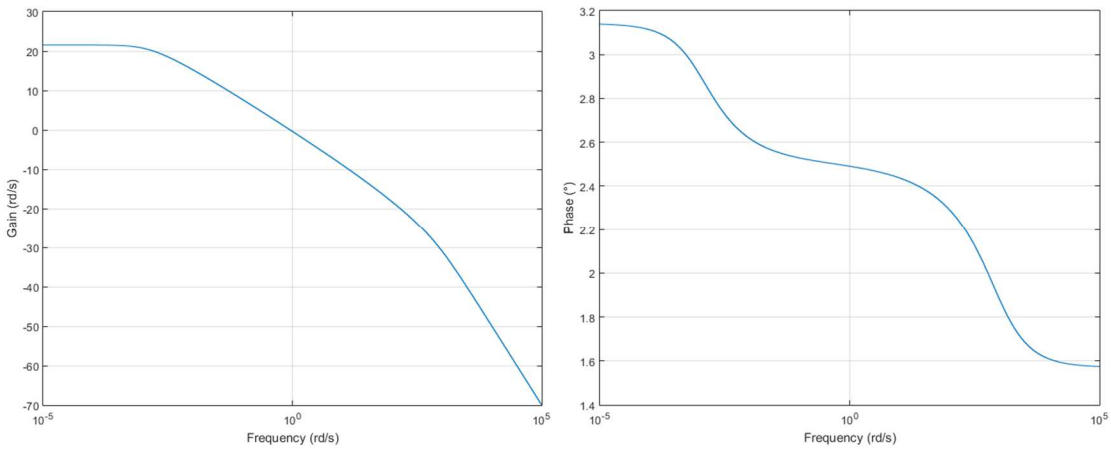

Figure – *Power law type behaviour of* $\frac{T(0,s)}{\varphi(0,s)}$